Temperature-dependent Brillouin light scattering spectra of magnons in yttrium iron garnet and permalloy

Kevin S. Olsson, Kyongmo An, Xin Ma, Sean Sullivan, Vijay Venu, Maxim Tsoi, Jianshi Zhou, Li Shi, and Xiaoqin Li

Phys. Rev. B **96**, 024448 — Published 28 July 2017

DOI: 10.1103/PhysRevB.96.024448

Temperature Dependent Brillouin Light Scattering Spectra of Magnons in YIG and Permalloy

Kevin S. Olsson[1], Kyongmo An[1], Xin Ma[1], Sean Sullivan[2], Vijay Venu[1], Maxim Tsoi[1], Jianshi Zhou[2], Li Shi[2, 3], and Xiaoqin Li[1,2,a)]

1. Department of Physics, Center of Complex Quantum Systems, The University of Texas at Austin, Austin, Texas 78712, USA
2. Texas Materials Institute, The University of Texas at Austin, Austin, Texas 78712, USA
3. Department of Mechanical Engineering, The University of Texas at Austin, Austin, Texas 78712, USA

In the field of spin caloritronics, knowledge of the magnon temperature is crucial. We investigate the temperature sensing capabilities of Brillouin light scattering (BLS), a technique which is commonly used in studying magnons. The magnon BLS spectra are characterized by three parameters: peak frequency, linewidth, and integrated intensity, each of which can be used for temperature sensing. The BLS spectra of magnons in both an insulator (yttrium iron garnet or YIG) and a metal (permalloy $Ni_{80}Fe_{20}$ or Py) are measured at different temperatures as the sample is uniformly heated. Unexpectedly, we find the temperature dependence of the BLS integrated intensity is opposite between YIG and Py. The mechanisms contributing to the temperature dependence of the three BLS spectra parameters are discussed and the temperature precision of each parameter is determined.

[a)] Author to whom correspondence should be addressed. E-mail: elaineli@physics.utexas.edu

In the emerging field of spin caloritronics, knowledge of spin transport, heat transport, and the coupling between these processes are essential[1, 2]. Different energy carriers, namely magnons, phonons, and electrons, are often driven out of thermal equilibrium which results in novel phenomena such as the spin Seebeck effect (SSE) and the spin-dependent Peltier effect[1-9]. Experimental techniques capable of measuring the effective temperature of a particular type of carrier may be used to disentangle the role of these carriers in spin caloritronic effects.

Typical techniques for measuring spin transport, such as those based on the spin-Hall effect, are not able to directly distinguish between different energy carriers[10]. Brillouin light scattering (BLS) is an inelastic light scattering technique that has been used to study magnons and acoustic phonons[11-15]. BLS measurements are not only able to distinguish magnons and phonons, but also able to distinguish between different modes of the carriers, such as between backward-volume and Damond-Eshbach magnon modes, and between longitudinal and transverse acoustic phonon modes[16-18]. The BLS spectra are generally characterized by three parameters: frequency, linewidth, and integrated intensity (further referred to simply as intensity). Previous BLS experiments have solely used the frequency shift to determine the temperature of magnons [11, 19]. In a different study, it was shown that frequency shift, linewidth, and intensity of BLS spectra of acoustic phonons in silicon all provide temperature sensing capabilities, though each probes different ranges of the acoustic phonon spectrum [16].

In this letter, we report systematic changes in BLS spectra of prototypical magnetic insulators and metals, i.e., yttrium iron garnet (YIG) and permalloy (Py) as the sample is uniformly heated. Changes in the BLS spectra arise from changes in the magnon population, which is used to define magnon temperature when the magnon chemical potential vanishes for the case of local thermal equilibrium. There are common features, as well as important differences, in temperature dependent BLS spectra in these two materials. The temperatures measured through the different parameters (central frequency, linewidth, and intensity) represent temperatures of different groups of magnons. The temperature dependence of the magnon frequency shift mainly follows the saturation magnetization temperature dependence and represents the average temperature of all magnon modes. The linewidth is determined by magnon scattering processes and shows different temperature dependence for YIG and Py likely due to different dominant scattering processes for the mode probed in BLS. The intensity depends on the magnon population of a specific mode and can be related to that mode's temperature after other factors (such as magneto-optical effects, saturation magnetization, and magnon diffusion non-equilibrium conditions) are carefully evaluated. The intensities are shown to have opposite temperature dependence in these two materials. This observation is contrary to the common, but over-simplified notion that a change in the BLS intensity directly correlates with a change in magnon population, as we demonstrate later in this paper. Finally, we evaluate the precision of each BLS spectra parameter as an effective magnon temperature sensor.

We first describe the samples and the measurement technique briefly. The two samples studied are a bulk, single crystal YIG sample, with [110] direction normal to the surface, and a polycrystalline Py thin film deposited on sapphire. In order to saturate the magnetization, a magnetic field of 50 mT is applied in the plane of the samples, perpendicular to the surface. The Curie temperatures of these materials are 560 K for YIG, and 550K to 870K for Py depending on the crystal structure[20, 21]. BLS spectra are

collected using a μBLS system, briefly described as follows [12, 19, 22]. A single frequency, linearly polarized 532 nm laser beam, normally incident on the sample, is focused using an objective lens (NA 0.70) to a spot size of approximately 1 μm in diameter. The polarization of the scattered light from magnons is perpendicular to that of the incident light due to the symmetry of the magneto-optic scattering coefficients[23, 24]. The same objective lens collects the back-scattered light and sends it to a Glan-Laser polarizer. This polarizer directs the magnon scattered light to a tandem, multi-pass Fabry-Pérot interferometer to collect the BLS spectra.

In the following, we uniformly heat the sample using a ceramic, resistive heater from approximately 300 K to 360 K in 10 K increments and observe systematic changes in BLS spectra. At each temperature, the samples equilibrate for 20 minutes, then fifteen one-minute spectra and four 5-minute spectra are collected at each temperature for YIG and Py, respectively. Only the anti-Stokes peaks are recorded which reduces the time necessary to sweep through the frequency region of interest. More sweeps can performed per unit time, leading to an increase in the signal to noise ratio. The magnon peaks are then fit to Lorentzian functions, shown in Figure 1. The averaged frequency, full width half maximum (FWHM) linewidths, and intensity from the multiple measurements are calculated using a weighted average $\bar{x} = (\sum x_i \sigma_i^{-2})/(\sum \sigma_i^{-2})$, where $\bar{x}$ and σ_i are the value and standard deviation determined from the Lorentzian fit. We then fit the average parameters to functions of temperature, using the simplest equation that fits the temperature dependence of the parameter over the measured temperature region. The fitting function is not necessarily the physically correct function to use, though for this calibration type of measurements, a physically correct temperature dependence is not required.

We note that the laser power used in the measurements was 8 mW. The laser induced local heating was simulated using a commercial software COMSOL following the method used in Ref [25]. The simulation shows that laser increased the local temperature by approximately 41 K in YIG and 20 K in Py when the stage temperature is 300 K. These temperatures are the average temperature increase in the volume measured by the laser. At a heater temperature of 360 K, the laser induced heating is 48 K for YIG due to temperature dependent thermal conductivity. For Py, the laser induced heating is 23 K at a stage temperature of 360K, since the thermal conductivity for Py is not a strong function of temperature. Full details of the simulations are provided in the Supplementary Materials[26].

Figure 2 a) and c) show that both the YIG and Py magnon frequencies follow a clear downward shift as stage temperature increases. To understand this temperature dependence, the magnon dispersion must first be described. For the bulk YIG sample, the dispersion of the magnon probed here is given by

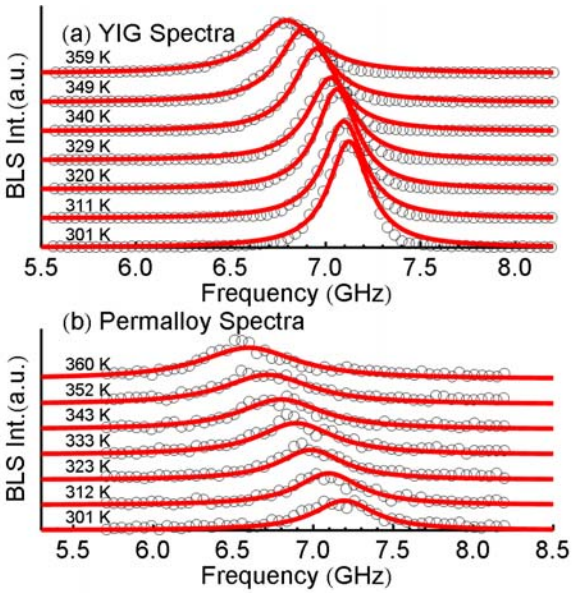

Fig. 1. BLS spectra of (a) YIG and (b) Py with increasing stage temperature. Black circles are the raw data points and the red curves are Lorentzian fits.

$$f_{\mathrm{m}}(q)=\frac{\gamma}{2\pi}\sqrt{\begin{matrix}[B+B_{\mathrm{a}}-\mu_0 N M_s(T)+Dq^2]\\ \times[B+B_{\mathrm{a}}-\mu_0 N M_s(T)\\ +Dq^2+\mu_0 M_s(T)]\end{matrix}} \quad (1)$$

where $\frac{\gamma}{2\pi}$ is the gyromagnetic ratio of 28.0 GHz T^{-1}, μ_0 is the permeability of free space, B_{a} is the anisotropy field of 1 mT [14], N is the calculated demagnetization factor along the applied field direction, D is the exchange stiffness constant of $(5.4 \pm 0.1) \times 10^{-17}$ T m^2 [27, 28], and M_s is the saturation magnetization. The YIG sample is approximately 1.2 x 1.5 x 0.5 mm in size. The wavevector of the magnon, q, is equal to the difference in the wavevectors of the scattered and incident light $\boldsymbol{q}=\boldsymbol{k_s}-\boldsymbol{k_i}$. In the backscattering geometry, $\boldsymbol{k_s}$ and $\boldsymbol{k_i}$ are antiparallel and approximately of the same magnitude. Thus, the wavevector of the magnon probed is $q=2|\boldsymbol{k_i}|=4\pi n/\lambda_i$, where n is the refractive index and λ_i is the wavelength of the incident light. YIG has a refractive index of 2.34, leading to the probed wavevector to be 5.53×10^7 m^{-1} [29]. The magnons probed in the Py thin film are the first (l=1) perpendicular standing spin wave (PSSW) mode, which has the following dispersion relation,

$$f_{\mathrm{m}}=\frac{\gamma}{2\pi}\sqrt{\begin{matrix}\left[B+\frac{2A}{M_s(T)}\left(\frac{\pi l}{t}\right)^2\right]\\ \times\left[B+\frac{2A}{M_s(T)}\left(\frac{\pi l}{t}\right)^2+\mu_0 M_s\right]\end{matrix}} \quad (2)$$

where A is the exchange constant equal to $(1.1 \pm 0.1) \times 10^{-11}$ J m^{-1}, $l=1$ is the thickness mode number, and t is the thickness of the film which is approximately 100 nm [30, 31]. The 1st order PSSW was chosen due its larger BLS intensity compared the other PSSW modes. For further details on the PSSW modes see the Supplementary Materials. The frequencies of both the YIG and Py magnons depend on the saturation magnetization, which has a well understood temperature dependence. YIG is a ferrimagnet where the temperature dependence of the magnetization follows the difference of two Brillouin functions for the two sub-lattices[32, 33]. Py is a ferromagnet where the magnetization decreases with increasing temperature following a single Brillouin function[19, 32]. These temperature dependent magnetizations lead to the decreasing frequencies of the magnons in YIG and Py. The YIG frequency is fit to a quadratic function of temperature $f_{\mathrm{YIG}}(T)=(2.58 \pm 0.03\ \mathrm{GHz})+(0.032 \pm 0.002\ \mathrm{GHz\ K^{-1}})T-(5.7 \pm 0.4 \times 10^{-5}\ \mathrm{GHz\ K^{-2}})T^2$. For Py, the frequency is fit to a linear function of temperature $f_{\mathrm{Py}}(T)=(10.22 \pm .07\ \mathrm{GHz})-(.0100 \pm .0002\ \mathrm{GHz\ K^{-1}})T$.

Once the temperature dependence of the frequency is determined, the frequency can be used to measure the temperature of the magnons with the appropriate considerations. The magnon frequency shift is due to a change in the saturation magnetization, which is related to the entire magnon population. In systems where local thermal equilibrium has been established for magnons, the chemical potential becomes zero and the magnon population can be directly related to a magnon temperature.

Many recently discovered interesting phenomena, such as the spin Seebeck effect, can only exist in non-equilibrium systems. The non-equilibrium conditions are intentionally created with a large thermal gradient or in parametric magnon pumping, and lead to a non-zero magnon chemical potential [25, 34-36]. In these systems, one can only relate the frequency to the magnon population, which follows the Bose-Einstein distribution determined by both temperature and chemical potential. Thus, the magnon frequency cannot necessarily be related to only the magnon temperature.

In this study, the probe laser introduced a local non-equilibrium while the effects of uniform heating are measured. If the temperature arise due to the laser heating is constant over the relevant temperature of range, a systematic error is introduced as a constant temperature increase and constant chemical potential. If one takes into account the temperature-dependent thermal and optical properties, the temperature rise due to laser heating differs by ~ 7 K at the stage temperatures of 300 K and 360 K. This change in the laser heating may change the chemical potential by a factor of up to ~ 7 K, which is small compared change in absolute temperature. This systematic error can be reduced by lowering the probe laser power. Aside from this systematic error, the frequency can be used to measure the magnon temperature with a precision of 0.06 K for YIG and 0.5 K for Py. These values are determined by taking the average of the uncertainties at each temperature and converting that value from GHz to temperature using the temperature dependent frequency fits in Fig. 2 (a) and (c).

The FWHM linewidths for both YIG and Py, shown in Fig 2 b) and d), increase with increasing temperature. The intrinsic linewidths for YIG and Py have been reported to be much smaller than those measured here[37, 38]. The laser linewidth (50 MHz), a large range of wave vectors collected by the objective, and the interferometer instrument spectral resolution all contribute to broadening of the linewidth measured in BLS spectra. The laser and instrument contributions do not change with sample heating, where the wave vector range does increase due to an increase in refractive index with temperature. The change in refractive index is on the order of 1%, leading the change in wave vector range to be negligible[16, 25].Thus, the increase in BLS linewidth observed results from an increase in the intrinsic linewidth. Magnon linewidth is expected to increase with increasing temperature due to increased magnon scattering. The dominant scattering process in YIG is magnon-magnon scattering. Previous measurements of the FMR linewidth of YIG show that magnon-magnon alone accurately describes the temperature dependence[39]. The magnons probed here exist in the wavevector region where both the dipole-dipole and exchange interactions are important. The dipole-dipole interaction mediates three-magnon scattering, which contributes a linear temperature dependence to the linewidth[39]. The exchange interaction leads to four-magnon scattering, contributing a quadric temperature dependence to the linewidth [40]. The YIG linewidth shows a clear superlinear temperature dependence, though it is not strictly quadratic. This observation agrees with the theory and previous studies of YIG suggesting that both three-magnon and four-magnon scattering make contributions to the linewidth [39, 40]. The Py linewidth also shows a

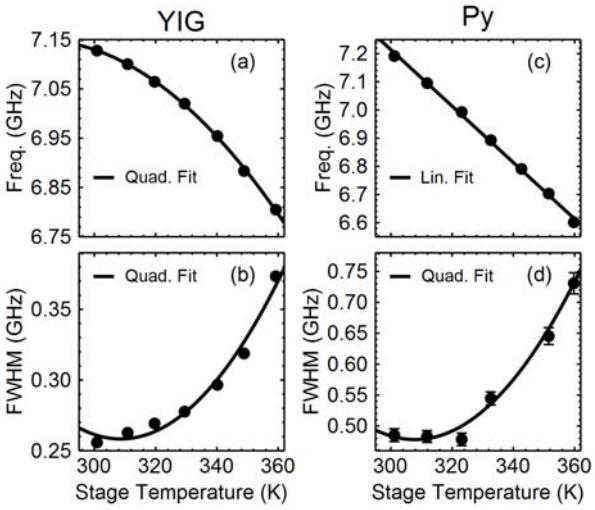

Fig. 2. BLS frequency and full width half maximum (FWHM) linewidth for (a, b) YIG and (c, d) Py. The frequency shifts in (a) and (c) decrease with increased stage temperature, following the magnetization dependence included in the respective magnon dispersion relations. The linewidths in (b) and (d) increase with increasing temperature as predicted by considering magnon scattering processes.

superlinear temperature dependence, though it is not as pronounced as for YIG. In Py, the electron-magnon scattering likely contributes to the linewidth and may change its overall temperature dependence. The effect of electron-magnon scattering on the magnon linewidth has yet to be investigated systematically [41]. If the system were in thermal equilibrium, the temperature precision using the linewidth is 0.07 K and 1 K, for YIG and Py respectively. These precisions are determined by converting the average of the uncertainties in the linewidth to a temperature using the following quadratic fits $w_{\mathrm{YIG}}(T) = (4.3 \pm 0.8\ \mathrm{GHz}) - (0.026 \pm 0.005\ \mathrm{GHz\ K^{-1}})T - (4.2 \pm 0.8 \times 10^{-5}\ \mathrm{GHz\ K^{-2}})T^2$ and $w_{\mathrm{perm.}}(T) = (9.4 \pm 2.0\ \mathrm{GHz}) - (0.058 \pm .012\ \mathrm{GHz\ K^{-1}})T + (9.4 \pm 1.8 \times 10^{-5}\ \mathrm{GHz\ K^{-2}})T^2$.

Finally, we evaluate intensity as a mode-specific magnon temperature sensor. The temperature of this mode uniquely determines the magnon population under local thermal equilibrium. Previous light scattering measurements of phonons, specifically Raman and BLS, have shown that the integrated intensity is proportional to the population of the probed phonon [16, 42]. Population, or occupancy of a mode, is, in fact, a more general concept that is valid under both equilibrium and non-equilibrium conditions. In the analysis below, we try to establish the correlation between BLS intensity with population of the measured magnon mode. The anti-Stokes BLS intensity of magnons can then be expressed by the following equation

$$I = I_0 \frac{\hbar \gamma M_s {\omega_0}^4}{2\pi {c_0}^4} |P|^2 n_m \qquad (3)$$

where I_0 is the incident intensity of the laser, $\hbar$ is the reduced Planck constant, ω_0 is the frequency of the incident light, c_0 is the speed of light in vacuum, P contains tensor coefficients describing how optical susceptibility relates to magnetization described in Ref [28], and n_m is the population of the probed magnon given by the Bose-Einstein distribution. The wavelengths of the incident and scattered light are assumed to be the same, which reduces the terms needed to described the BLS intensity[28].

Figure 3 a) and 3 c) show that that BLS intensity for YIG and Py have opposite dependence on temperature. The only temperature dependent terms in equation (3) are M_s, P, and n_m. The saturation magnetization at each temperature is calculated by converting the measured frequency value to a saturation magnetization value through the dispersion relations. In the magnon dispersion relations, the saturation magnetization is assumed to be the only temperature dependent term. Fitting the frequencies to dispersion relations with magnetization temperature dependence with polynomials of order $T^{5/2}$ for YIG and $T^{3/2}$ for Py results in excellent fits, suggesting the temperature dependence of the other terms is weak in the observed temperature range [32, 43].

The intensities at each temperature are then divided by the calculated saturation magnetization to remove its temperature dependence from the intensity. The Bose-Einstein distribution is calculated from the magnon frequency and temperature of the stage. The saturation magnetization corrected BLS intensity can then be compared to the calculated Bose-Einstein distribution to evaluate if the tensor coefficients are temperature dependent. Fig. 3 b) and d) show the normalized, saturation magnetization corrected BLS intensity and the normalized, Bose-Einstein magnon distribution for both YIG and Py. To normalize the corrected BLS intensity, the values are divided by linear and quadratic fits of the corrected intensity at 300 K for YIG and Py, respectively. The Bose-Einstein distributions for each material are normalized to their calculated values at 300 K as well. The Bose-Einstein distributions include a temperature dependent offset temperatures, $T_o(T) = 5.35\ \mathrm{K} + 0.116T$ for

YIG and $T_o(T) = 5.049\ \mathrm{K} + 0.0049T$ for Py, to account for the laser induced heating. We confirm that the local heating from the probe laser does not change the Bose-Einstein distributions appreciably (See the Supplementary Materials for a comparison of different Bose-Einstein distributions). The corrected YIG intensity follows the Bose-Einstein distribution, suggesting tensor coefficients in P are relatively constant in the temperature interval measured. In Py, the normalized corrected BLS intensity deviates from the calculated Bose-Einstein distribution. We suggest two possible contributing factors to this deviation. One is the temperature dependence of the P tensor coefficients in Py, and the other is the non-equilibrium of the PSSW mode. Further study is necessary to identify the relative contributions of the possible factors to the observed deviation. The temperature precision for intensity-based sensing was determined to be 5 K and 1 K, for YIG and Py respectively, from the average uncertainty of the intensity and the fits, $I_{\mathrm{YIG}}(T) = -(0.30 \pm 0.17) + (4.3 \pm 0.5 \times 10^{-3})T$ and $I_{\mathrm{perm.}}(T) = (46 \pm 7) + (.30 \pm 0.04)T + (5.0 \pm 0.6 \times 10^{-4})T^2$.

All three parameters measured by BLS can be used as empirical temperature sensors following a uniform heating calibration as described here. As discussed above, these parameters can only be related to the magnon temperature under local equilibrium conditions, when the magnon chemical potential is zero. The temperatures measured through each parameter are not necessarily equivalent. We now discuss what the temperatures measured by each parameter represent in equilibrium. The temperature measured through the frequency shift is related to the magnetization, which reflects the sum of all magnons existing in the sample. Thus, the temperature measured by the frequency is related to the average magnon population. The linewidth temperature dependence is determined by various magnon scattering processes. The linewidth is proportional to the temperature of the magnons and other carriers that scatter with the magnon being probed in the BLS spectrum[40]. Finally, the corrected BLS intensity temperature dependence is related to the magnon population just for the magnon mode being probed. In local thermal equilibrium the magnon population is determined by the Bose-Einstein distribution, and thus offers the possibility to uniquely measure the temperature of a single magnon mode, as similarly concluded for phonons in a previous study [16]. It should be noted the corrected BLS intensity can only measure relative temperature changes, not absolute temperatures. This is due to the sensitive nature of the tandem Fabry-Pérot interferometer. Slight variations in the

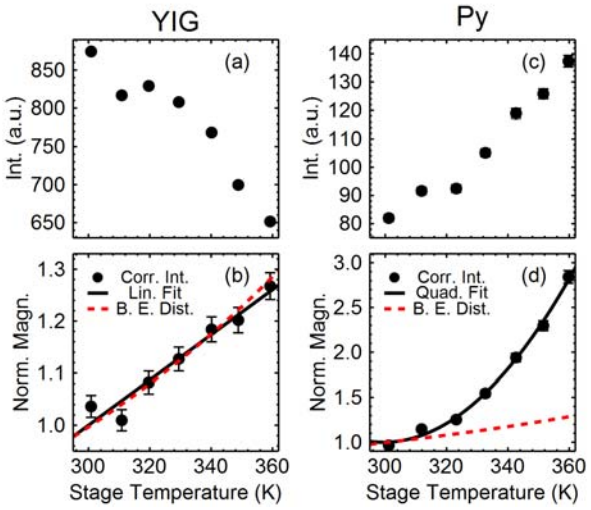

Fig. 3. The BLS intensity for (a) YIG decreases with increasing temperature, suggesting that the magnetization term is dominant. (c) The Py BLS intensity increases with increasing temperature, suggesting that the magnet-optic terms are dominant. The normalized Bose-Einstein distribution and normalized, magnetization corrected BLS intensity for (b) YIG and (d) Py. The Bose-Einstein distribution is found from the respective magnon frequencies and normalized by the value at 300 K. The corrected BLS intensity is found by dividing BLS intensity by the magnetization, which is calculated from the frequency shift and magnon dispersion relations. The corrected intensity is then normalized by the value at 300 K.

interferometer's cavity spacing cause the transmission to significantly change between different sets of measurements even when a strict, systematic alignment procedure is followed. Ultimately this sensitivity to alignment makes absolute BLS intensity measurements difficult, if not impossible. In non-equilibrium systems, the magnon distribution cannot be described by the Bose-Einstein distribution with temperature as the single parameter. In this case, the concept of magnon temperature is ill defined. Nevertheless, the three parameters characterizing BLS spectra may still be correlated to a magnon populatoin of different magnon groups[25].

In summary, the temperature dependences of the several parameters associated with magnon BLS spectra were studied in YIG and Py. For both samples the frequency and linewidth followed the trends expected based on the temperature dependent magnetization and magnon scattering, respectively. The integrated intensity can be used as a mode specific magnon temperature sensor once other temperature dependent effects are properly taken into account. These results indicate that changes in the raw BLS intensity cannot always be used to as a direct measure of changes in the magnon population. Finally, the temperature precisions for YIG and Py, respectively, were measured to be 0.06 K and 0.5 K for the frequency, 0.07 and 1 K for the linewidth, and 5 K and 1 K for the magnetization corrected intensity.

Acknowledgements:
Financial support for K. O (partial support), K. A., X. M., and X. L are provided by SHINES, an Energy Frontier Research Center funded by the U.S. Department of Energy (DoE), Office of Science, Basic Energy Science (BES) under award # DE-SC0012670. Partial support for K. O and support for SS and LS are provided by National Science Foundation (NSF) Thermal Transport Processes Program under Grant No. CBET-1336968.

References

1 G. E. W. Bauer, E. Saitoh, and B. J. van Wees, Nature Materials **11**, 391 (2012).
2 S. R. Boona, R. C. Myers, and J. P. Heremans, Energy & Environmental Science **7**, 885 (2014).
3 C. M. Jaworski, J. Yang, S. Mack, D. D. Awschalom, J. P. Heremans, and R. C. Myers, Nature Materials **9**, 898 (2010).
4 K. Uchida, et al., Nature Materials **9**, 894 (2010).
5 M. Johnson, Solid State Commun **150**, 543 (2010).
6 J. Flipse, F. L. Bakker, A. Slachter, F. K. Dejene, and B. J. van Wees, Nature Nanotechnology **7**, 166 (2012).
7 M. Hatami, G. E. W. Bauer, Q. F. Zhang, and P. J. Kelly, Phys Rev B **79**, 174426 (2009).
8 A. Kehlberger, et al., Phys Rev Lett **115**, 096602 (2015).
9 J. Xiao, G. E. W. Bauer, K. Uchida, E. Saitoh, and S. Maekawa, Phys Rev B **81**, 214418 (2010).
10 Y. Kajiwara, et al., Nature **464**, 262 (2010).
11 M. Agrawal, V. I. Vasyuchka, A. A. Serga, A. D. Karenowska, G. A. Melkov, and B. Hillebrands, Phys Rev Lett **111**, 107204 (2013).
12 V. E. Demidov, S. O. Demokritov, B. Hillebrands, M. Laufenberg, and P. P. Freitas, Applied Physics Letters **85**, 2866 (2004).
13 V. E. Demidov, S. Urazhdin, H. Ulrichs, V. Tiberkevich, A. Slavin, D. Baither, G. Schmitz, and S. O. Demokritov, Nature Materials **11**, 1028 (2012).
14 J. R. Sandercock, Phys Rev Lett **28**, 237 (1972).
15 J. R. Sandercock and W. Wettling, Solid State Commun **13**, 1729 (1973).
16 K. S. Olsson, N. Klimovich, K. An, S. Sullivan, A. Weathers, L. Shi, and X. Q. Li, Applied Physics Letters **106**, 051906 (2015).

[17] G. Srinivasan, J. G. Booth, and C. E. Patton, IEEE Transactions on Magnetics **23**, 3718 (1987).
[18] A. A. Stashkevich, et al., J Appl Phys **104**, 093912 (2008).
[19] D. R. Birt, K. An, A. Weathers, L. Shi, M. Tsoi, and X. Q. Li, Applied Physics Letters **102**, 082401 (2013).
[20] L. F. Yin, et al., Phys Rev Lett **97**, 067203 (2006).
[21] V. Cherepanov, I. Kolokolov, and V. Lvov, Phys Rep **229**, 81 (1993).
[22] K. An, D. R. Birt, C. F. Pai, K. Olsson, D. C. Ralph, R. A. Buhrman, and X. Q. Li, Phys Rev B **89**, 140405 (2014).
[23] B. A. Auld and D. A. Wilson, J Appl Phys **38**, 3331 (1967).
[24] P. A. Fleury and R. Loudon, Phys Rev **166**, 514 (1968).
[25] K. An, et al., Phys Rev Lett **117**, 107202 (2016).
[26] See Supplemental Material at @@URL inserted by Publisher@@
[27] S. Klingler, A. V. Chumak, T. Mewes, B. Khodadadi, C. Mewes, C. Dubs, O. Surzhenko, B. Hillebrands, and A. Conca, J Phys D Appl Phys **48**, 015001 (2015).
[28] W. Wettling, M. G. Cottam, and J. R. Sandercock, Journal of Physics C-Solid State Physics **8**, 211 (1975).
[29] G. B. Scott, Lackliso.De, and J. L. Page, Phys Rev B **10**, 971 (1974).
[30] C. Bayer, et al., Phys Rev B **72**, 064427 (2005).
[31] N. Smith, D. Markham, and D. Latourette, J Appl Phys **65**, 4362 (1989).
[32] D. D. Stancil and A. Prabhakar, *Spin waves : theory and applications* (Springer, New York, 2009).
[33] P. Hansen, P. Roschmann, and W. Tolksdorf, J Appl Phys **45**, 2728 (1974).
[34] S. O. Demokritov, V. E. Demidov, O. Dzyapko, G. A. Melkov, A. A. Serga, B. Hillebrands, and A. N. Slavin, Nature **443**, 430 (2006).
[35] A. A. Serga, et al., Nat Commun **5**, 3452 (2014).
[36] O. Dzyapko, V. E. Demidov, S. O. Demokritov, G. A. Melkov, and A. N. Slavin, J Appl Phys **101**, 09c103 (2007).
[37] R. C. Lecraw, E. G. Spencer, and C. S. Porter, Phys Rev **110**, 1311 (1958).
[38] Y. L. Zhao, Q. Song, S. H. Yang, T. Su, W. Yuan, S. S. P. Parkin, J. Shi, and W. Han, Scientific reports **6**, 22890 (2016).
[39] A. N. Anisimov and A. G. Gurevich, Fizika Tverdogo Tela **18**, 38 (1976).
[40] A. G. Gurevich and G. A. Melkov, *Magnetization oscillations and waves* (CRC Press, Boca Raton, 1996).
[41] V. P. Silin and A. Z. Solontsov, Soviet Phyics JETP **62**, 829 (1985).
[42] T. R. Hart, R. L. Aggarwal, and B. Lax, Phys Rev B **1**, 638 (1970).
[43] I. H. Solt, J Appl Phys **33**, 1189 (1962).